

Rubrique

## Modeling the dynamics of cell-sheet : From Fisher-KPP equation to bio-mechano-chemical systems

### Fisher-KPP equation to study some predictions on the injured cell sheet

Mekki Ayadi <sup>1</sup> — Abderahmane Habbal <sup>2</sup> — Boutheina Yahyaoui <sup>1</sup>

<sup>1</sup> Tunis El Manar University, National Engineering School of Tunis  
ENIT-LAMSIN BP 37, 1002 Tunis, LR 95-ES-20  
Tunisia

mekki.ayadi@enis.rnu.tn

boutheinayahyaoui@hotmail.fr

<sup>2</sup> INRIA, 2004 route des lucioles-BP 93

06902 Sophia Antipolis Nice cedex

France

Abderrahmane.HABBAL@unice.fr



**RÉSUMÉ.** Dans le cadre de la cicatrisation d'un feuillet cellulaire, nous avons étudié la validité des modèles de réaction-diffusion de type Fisher-KPP pour la simulation de la migration de feuillets cellulaires. Afin d'étudier la validité de ce modèle, nous avons effectué des observations expérimentales sur les monocouches de cellules MDCK. Les vidéos obtenues permettent, après segmentation et binarisation, d'obtenir avec précision les variations d'aire et de profils de fronts de cicatrice. Nous nous sommes intéressés à comparer les variations des fronts calculés à celles des fronts expérimentaux, après une étape de calage des paramètres.

**ABSTRACT.** This paper is devoted to study some predictions on the injured cell sheet mainly based on reaction-diffusion equations. In the context of healing of cell sheet, we investigated the validity of the reaction-diffusion model of Fisher-KPP type for simulation of cellular sheets migration. In order to study the validity of this model, we performed experimental observations on the MDCK cell monolayers. The obtained videos allow to obtain, after segmentation and binarization, the variations of area and of scar fronts profiles with good accuracy. We were interested in comparing the calculated variations of fronts to those experimental fronts, after a step of calibration parameters.

**MOTS-CLÉS :** Cellules MDCK, Fisher-KPP, simulation 2D, dynamique cellulaire, coefficient de diffusion  $D$ , taux de prolifération  $r$ .

**KEYWORDS :** MDCK, Fisher-KPP, wound edge dynamics, diffusion coefficient  $D$ , proliferation rate  $r$ , activation, inhibition.



## 1. Introduction

"Medicine and mathematics, this may seem a bold rapprochement. And yet ... medical imaging provides a unique way to access the inaccessible, the shape and function of internal organs from living human body, without being invasive. Thanks to medical images, physicians and surgeons can see what remains invisible during an examination with the naked eye. What is also visible, it is the essential role of mathematics and computing not only in the formation of these images, but also in their use".

Grégoire Malandain [1].

Modeling cell dynamics, for studying the cell-sheet wound healing, is a subject of great importance and at the intersection of three major fields of science. In fact, biology for the part of experimental measurements and filtering data, mechanical for modeling the movement of the tissue and its effect on wound healing and mathematical and numerical modeling to quantify biological and mechanical quantities previously mentioned.

Modeling bio-mechano-chemical behavior coupled with complex biological systems, such as the formation of a pattern in embryogenesis, modeling of tumor growth and wound healing, is in mathematical term won by partial differential equations of reaction-diffusion type [2]. This family of equations is well suited to describe in time and in space changes that occur within the cell population and the production of migration and proliferation. Both mechanisms are most important during wound healing. Basically, the diffusion cells is related to their roving, while the reaction is related to proliferation. Reaction-diffusion equations coupled to mechanics with viscoelastic behavior, take into account haptotaxis and haptokinesis of cell movement [3].

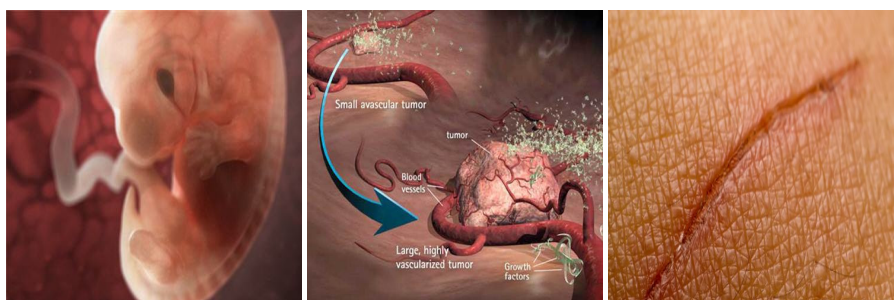


**Figure 1.** Formation of a pattern in embryogenesis, tumor growth and wound healing, <http://www.linternaute.com/science/biologie/dossiers/07/cerveau-sexe/page4.jpg>, <http://www.santevitalite.be/wp-content/uploads/2012/12/Croissance-tumorale.jpg>, <https://www.simplyscience.ch/system/html/Croute-01b7ea33.jpg>

In this study, we consider a particular aspect of wound healing, namely that relative to the flow of monolayers of wounded epithelial cells of Madin-Darby Canine Kidney (MDCK) [4, 5]. The population of cells in epithelial monolayers, also called cellular sheet can be considered as a two-dimensional structure. After creating a wound, the cells begin to regrowth in order to fill the empty space. Although wound closure involves biochemical and biomechanical process, still far from being understood, which are distributed

throughout the monolayer, particular attention was paid to changes in the front. Moreover, the effects of migration activators of HGF (Hepatocyte Growth Factors) type [6] and the effects of inhibitors of PI3K (phosphoinositide 3-kinase) type were taken into account in an experimental test campaign.

To our knowledge, J.D. Murray published during the 2000s an interesting study describing the relationship between biology and mathematics in his book entitled *Mathematical Biology* in two parts [7], [8]. He proposes a vision of a mathematician to study reaction-diffusion models that describe the problems of interactions between biological, chemical and mechanical phenomena. Mathematical biology allows to pass from dynamic analysis of cells to a mechano-biochemical system governed by reaction-diffusion equations, coupled to mechanics equations with a visco-elastic behavior, as well as to explain the phenomena of chemotaxis and haptotaxis among other characteristics of cell movement [9, 10, 11].

In order to build a powerful mechanical model for modeling biological problems difficult to solve, we refer interested readers to the articles [12, 13, 14, 15]. The authors of these articles consider that healing is largely a mechanical process where the chemical effect simply acts to increase the overall behavior. Moreover, in the works of Maini, Olsen and Sherratt published in [3], [16], [17] presented a complete coupled model whose basic variables are cell density  $n$ , the density of ECM  $\rho$  and the displacement of tissue  $u$ , see the following equations.

$$\frac{\partial n}{\partial t} + \text{div}[n \frac{\partial u}{\partial t} + \chi(\rho)n \nabla \rho - D(\rho) \nabla n] = rn(1 - n), \quad (1.1)$$

$$\frac{\partial \rho}{\partial t} + \text{div}[\rho \frac{\partial u}{\partial t}] = \varepsilon n(1 - \rho), \quad (1.2)$$

$$\text{div}(\sigma) = \rho s u, \quad (1.3)$$

where

- $\text{div}(n \frac{\partial u}{\partial t})$  represents the passive convection, while,  $\text{div}(\chi(\rho)n \nabla \rho)$  represents the haptotaxis phenomenon,  $(-\text{div}(D(\rho) \nabla n))$  represents the haptokinesis phenomenon and  $rn(1 - n)$  represents the cell proliferation,
- $\text{div}(\rho \frac{\partial u}{\partial t})$  represents the passive convection, while  $\varepsilon n(1 - \rho)$  represents the ECM biosynthesis and the degradation of cells fibroblast,
- $\sigma = \sigma_{ECM} + \sigma_{cell}$  with  $\sigma_{ECM} = \mu_1 \frac{\partial \varepsilon}{\partial t} + \mu_2 \frac{\partial \Theta}{\partial t} I + \frac{E}{1+\nu} (\varepsilon(u) + \frac{\nu}{1-2\nu} \Theta I)$  represents the viscous and elastic forces, while,  $\sigma_{cell} = cnI$  represents the traction forces,  $\varepsilon(u) = \frac{1}{2}(\nabla u + \nabla u^T)$  is the strain tensor and  $\Theta = \text{tr}(\varepsilon)$  is the dilatation of the matrix material.

Many scientific articles describe in detail this model. These include for example that of Perelson and *all*, [18]. In this paper is shown how the above equations are found as well as their numerical implementation. In the article [19], Sherratt offers monodimensional and another bidimensional model which include only biomechanical coupling to describe cellular dynamics during healing embryonic dermal wounds. In [20], Goto uses mechanochemical model, which is a simplified version of the full model mentioned above, for the formation of a somite to better understand the role played by the mechanical aspects of the cells and the extracellular matrix (ECM) in the somitogenesis.

## 2. Material and methods

### 2.1. Mathematical method

In what follows, the mechanical and chemical effects are neglected ; only the biological effect is considered. Hence, the full coupled model (1.1) – (1.3) reduces to the Fisher-KPP equation.

$$n_t - D\Delta n + g(n) = 0, \quad (x, y) \in \Omega, \quad 0 < t \leq T, \quad (2.1)$$

with the initial condition

$$n(x, y, 0) = n_0(x, y), \quad (x, y) \in \Omega, \quad (2.2)$$

and with the boundary conditions

$$n = 1, \quad \text{on } \Gamma_D, \quad (2.3)$$

$$\frac{\partial n}{\partial y} = 0, \quad \text{on } \Gamma_N, \quad (2.4)$$

where  $g(n) = -rn(1 - n)$ ,  $\Omega$  is a bounded rectangular open set of  $\mathbb{R}^2$ ,  $\Gamma_D$  and  $\Gamma_N$  are respectively the vertical sides and the horizontal sides of  $\Omega$ , see Figure 2 [21],  $D$  and  $r$  are positive constants and stand for the cell diffusion coefficient and the cell proliferation rate respectively.

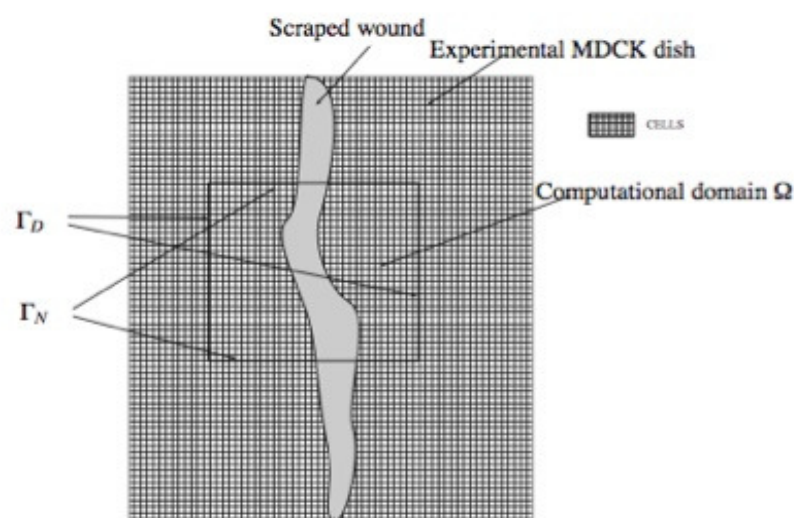


**Figure 2.** A neighborhood  $\Omega$  of the wound.

## 2.2. Experimental method

The experimental method has been presented as following : we conducted five experiments for healing wound, which give five data sets, each composed of 360 images. From each set, we extract a series of 120 two-dimensional images of  $1392 \times 1040$  pixels coded on 2 bytes, which corresponds to a step time of 6 minutes between two consecutive images. The tests are classified as follows :

- Assay I (Seq5) : considered as a control test or as a reference test (in which neither activator nor inhibitor migration was used).
- Assay II (Seq2) and Assay III (Seq4) : control test + HGF activator.
- Assay IV (Seq3) and Assay V (Seq6) : control test + inhibitor.

We recorded biological videos filming the various stages of wound closure. The videos were then segmented to obtain raw images, then they have been binarized to obtain images ready to deal with : the experimental density of cells, denoted  $n_{exp}$ , is provided. Using this density, we have successfully implemented experimental area of the wound :

$$W_{exp}(t) = \int_{\Omega} (1 - n_{exp}(x, y, t)) dx dy. \quad (2.5)$$

These experimental results were compared to numerical results related to the numerical solution, denoted  $n_{num}$ , of the KPP-Fisher equation discretized in space using a finite difference scheme of order two and in time using the Crank Nicolson scheme with Splitting. It is more precisely to minimize with respect to parameters  $r$  and  $D$  the following two costs

$$J_U(r, D) = \int_{[T_0, T]} \int_{\Omega} |n_{num}(x, y, t) - n_{exp}(x, y, t)| dx dy dt, \quad (2.6)$$

$$J_A(r, D) = \int_{[T_0, T]} |W_{num}(t) - W_{exp}(t)| dt. \quad (2.7)$$

The first cost is the norm of the error between the numerical solution and the experimental solution, while the second cost is the norm of the error between the numerical area and the experimental area. Figure (3) below shows the surfaces cost  $J_U$  and  $J_A$  in terms of parameters  $r$  and  $D$ .

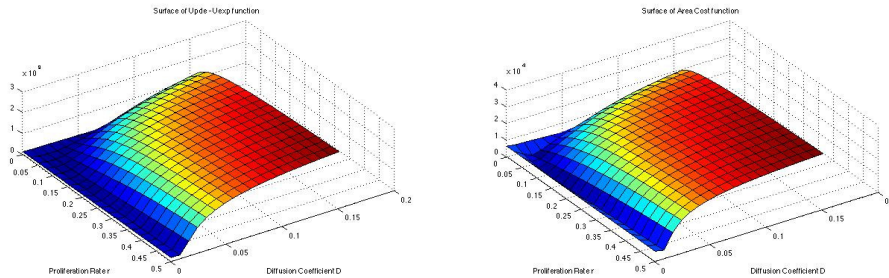


**Figure 3.** Cost functions of surfaces  $J_U$  and  $J_A$  function of parameters  $(r, D)$

The numerical results on the area of the wound depending on time, obtained by Habbal *et al*, in the absence of activation and inhibition, published in [21], are shown in the following figures. The blue curve represents the experimental area variation of the wound

with respect to time, while, the red curve represents the numerical area of the wound with respect to time.

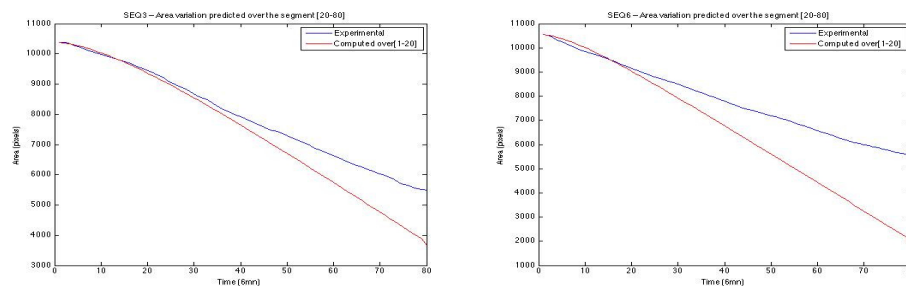


**Figure 4.** The curves show the area of the wound depending on time for sequences 3 and 6 respectively.

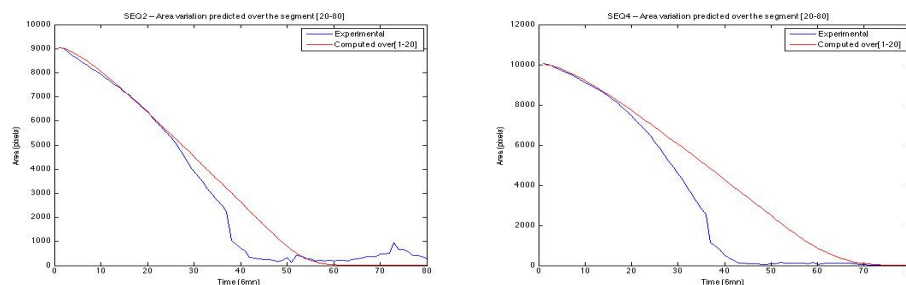


**Figure 5.** The curves show the area of the wound depending on time for sequences 2 and 4 respectively.

The above curves show that if the numerical area well approach the experimental area at the beginning of healing, this approximation is not at all satisfactory in the remaining time. To improve this approximation, we made recourse to activation and inhibition operations which are the novelty of this paper and the object of the following section.

From numerical point of view, activation and inhibition operations are taken into account by assuming that parameters  $D$  and  $r$  vary over time in a very precise manner. Charles Hansen suggested, after long studies on the choice of parameters including biological problems such as the prediction of cytotoxic drug interactions with DNA [22], a variation in sigmoid shape.

### 3. Results

#### 3.1. Numerical Results

A sigmoid function, see [23, 24], is a S-shaped curve whose general expression is  $\phi(t) = \frac{k}{1 + \alpha \exp(-\lambda t)}$ . Its growth is slow at first, then accelerates strongly before slowing to end up not grow. In a first step, we have chosen to vary only parameter  $D$  over time :

$$D(t) = \frac{k}{1 + \alpha \exp(-\lambda t)}, \quad \lim_{t \rightarrow +\infty} D(t) = k$$

The numerical results are very satisfactory as shown in the following figures :

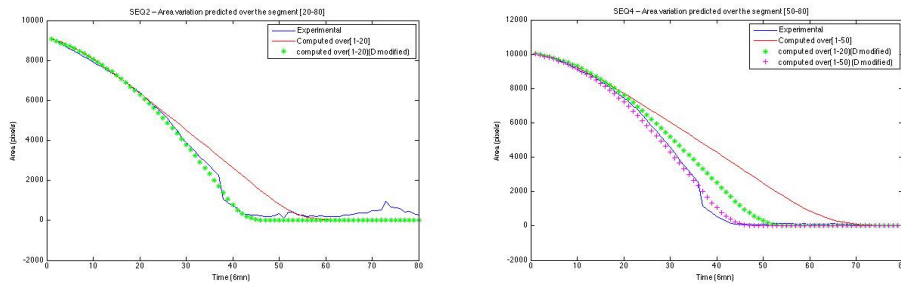


**Figure 6.** The curves show the numerical areas obtained after activation with sequences 2 and 4, respectively

These numerical results with the optimal settings :  $k_2^* = 2.00e - 02$ ,  $\lambda_2^* = 2.49e - 02$ ,  $\alpha_2^* = 3.00e + 01$ ,  $r_2^* = 2.26e - 01$  for the second sequence and  $k_4^* = 2.00e - 02$ ,  $\lambda_4^* = 4.00e - 02$ ,  $\alpha_4^* = 6.00e + 01$ ,  $r_4^* = 2.21e - 01$  for the fourth sequence, realize the minimum of the error between the experimental and the numerical area. This optimization operation has been performed using the Matlab function "fmincon".

We are now interested in choosing a sigmoid pattern compatible with the inhibition operation to improve the numerical area for sequences 3 and 6.

$$D(t) = \frac{3k}{2} - \frac{k}{1 + \alpha \exp(-\lambda t)}, \quad \lim_{t \rightarrow +\infty} D(t) = \frac{k}{2}$$

Numerical results obtained are less satisfactory than those obtained in the case of activation as shown in Figure 7.

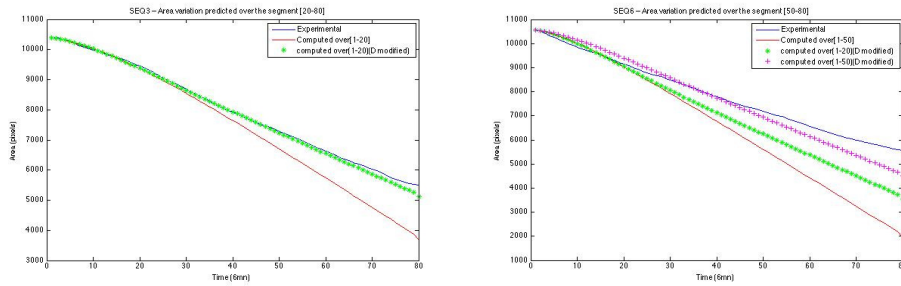


**Figure 7.** The curves show the numerical areas obtained after inhibition with sequences 3 and 6 respectively

These numerical results, illustrated by the green curve, are obtained with the optimal settings :  $k_3^* = 1.32e - 02$ ,  $\lambda_3^* = 4.00e - 02$ ,  $\alpha_3^* = 3.00e + 01$ ,  $r_3^* = 2.99e - 02$  for the third sequence and  $k_6^* = 2.00e - 02$ ,  $\lambda_6^* = 4.00e - 02$ ,  $\alpha_6^* = 3.00e + 01$ ,  $r_6^* = 2.93e - 02$  for the sixth sequence. If the result obtained with inhibition and sequence 3 is more or less acceptable, that of the sequence 6 is not at all acceptable. Hoping to get better results, we decided to also vary the parameter  $r$  over time.

Drawing on results in Figure 7, we choose the following variations of parameters  $r$  and  $D$  with respect to time :

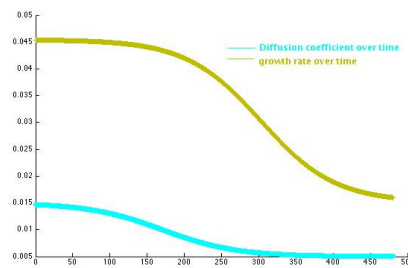


**Figure 8.** Diffusion and proliferation coefficients time-dependent

Numerical results obtained become very satisfactory as shown in the following figures.



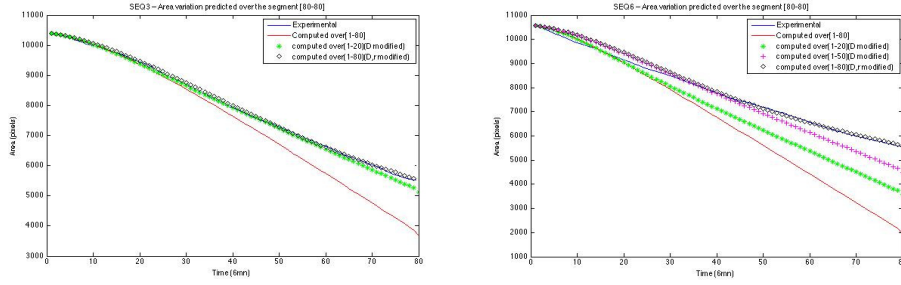


**Figure 9.** The curves show the numerical areas obtained after inhibition with sequences 3 and 6 respectively

In both cases, the numerical curve (shown in black diamonds) coincides so much with the experimental curve (shown in continu blue line) that one can not see the latter. These numerical results are obtained with the optimal settings :  $k_{D3}^* = 2.00e - 02$ ,  $\lambda_{D3}^* = 4.00e - 02$ ,  $\alpha_{D3}^* = 3.4631e + 03$ ,  $k_{r3}^* = 1.72e - 02$ ,  $\lambda_{r3}^* = 1.00e - 02$ ,  $\alpha_{r3}^* = 12.1045$  for the third sequence and  $k_{D6}^* = 2.00e - 02$ ,  $\lambda_{D6}^* = 4.00e - 02$ ,  $\alpha_{D6}^* = 3.4631e + 03$ ,  $k_{r6}^* = 1.93e - 02$ ,  $\lambda_{r6}^* = 1.05e - 02$ ,  $\alpha_{r6}^* = 14.5041$  for the sixth sequence.

### 3.2. Theoretical Results

We are interested in this section to the theoretical study of Fisher-KPP equation when the diffusion coefficient  $D$  and the proliferation rate  $r$  vary over time : estimate the difference of the wound surface variation for the two cases, constant and time-dependent. For a similar study we refer to [25] and [26].

#### 3.2.1. Diffusion and proliferation coefficients time-dependent

Consider the two following problems :

$$(P_1) \begin{cases} \partial_t u_1 = D \Delta u_1 + r u_1 (1 - u_1), & (x, y, t) \in \Omega \times (0, T], \\ u_1(x, y, 0) = u_{1,0}(x, y), & (x, y) \in \bar{\Omega}, \\ u_1(x, y, t) = u_H(x, y, t), & (x, y, t) \in \Gamma_D \times (0, T], \\ \frac{\partial u_1}{\partial n}(x, y, t) = g(x, y, t), & (x, y, t) \in \Gamma_N \times (0, T]. \end{cases} \quad (P_1.1)$$

$$(P_2) \begin{cases} \partial_t u_2 = D(t) \Delta u_2 + r(t) u_2 (1 - u_2), & (x, y, t) \in \Omega \times (0, T], \\ u_2(x, y, 0) = u_{2,0}(x, y), & (x, y) \in \bar{\Omega}, \\ u_2(x, y, t) = u_H(x, y, t), & (x, y, t) \in \Gamma_D \times (0, T], \\ \frac{\partial u_2}{\partial n}(x, y, t) = g(x, y, t), & (x, y, t) \in \Gamma_N \times (0, T]. \end{cases} \quad (P_2.1)$$

**Lemme 3.1** Suppose that  $u_{1,0}, u_{2,0} \in H^1(\Omega)$ ,  $u_1 \in L^2(0, T; H^2(\Omega))$  and  $u_2 \in L^2(0, T; H^1(\Omega))$ , then we have the following estimate :

$$\|u_2 - u_1\|_{0,\Omega} \leq e^{L(t)} \|u_{2,0} - u_{1,0}\|_{0,\Omega} + e^{L(t)} \int_0^t e^{L(s)} \left[ \|D(s) - D\| \|\Delta u_1\|_{0,\Omega} + |\Omega| |r(s) - r| \right] ds. \quad (3.1)$$

The area of the wound at the instant  $t$ , defined by the formula (2.5), yields

$$\begin{aligned} |W_2(t) - W_1(t)| &\leq \int_{\Omega} |u_2 - u_1| dx \\ &\leq \sqrt{|\Omega|} \|u_2 - u_1\|_{0,\Omega}, \end{aligned}$$

where  $|\Omega|$  denotes the measure of  $\Omega$ .

### 3.2.2. Estimate of $\|\Delta u_1\|_{0,\Omega}$

We are now seeking to estimate  $\|\Delta u_1\|_{0,\Omega}$  as a function of the data  $u_{1,0}$ ,  $D$  and  $r$ . In order to be reduced to a homogeneous problem, we make the following change of unknown :  $w_1 = 1 - u_1$  in the problem  $(P_1)$ . The new unknown  $w_1$  is then the solution to the following problem :

$$(P_4) \begin{cases} \frac{\partial w_1}{\partial t}(x, y, t) - D\Delta w_1(x, y, t) + rw_1(1 - w_1) = 0, & (x, y, t) \in \Omega \times ]0, T[, \\ w_1(x, y, 0) = w_0(x, y) = 1 - u_{1,0}, & (x, y) \in \bar{\Omega}, \\ w_1(x, y, t) = 0, & \text{dans } \Gamma_V \times [0, T], \\ \frac{\partial w_1}{\partial n}(x, y, t) = 0, & \text{dans } \Gamma_H \times [0, T]. \end{cases}$$

**Lemme 3.2** Suppose that  $u_{1,0} \in H^1(\Omega)$  and  $u_1 \in L^2(0, T; H^2(\Omega))$ , we get the following estimate

$$\|\Delta u_1\|_{0,\Omega}^2 \leq 2 \sum_{n=1}^{+\infty} \lambda_n^2 \left( \|1 - u_{1,0}\|_{0,\Omega}^2 e^{-2D\lambda_n t} + r^2 |\Omega| t \int_0^t e^{-2D\lambda_n(t-s)} ds \right), \quad (3.2)$$

where  $(\lambda_n)_{n \in \mathbb{N}^*}$  are eigenvalues of the following eigenvalue problem :

$$(P_5) \begin{cases} -\Delta v = \lambda v, & \text{in } \Omega, \\ v = 0, & \text{on } \Gamma_V, \\ \frac{\partial v}{\partial n} = 0, & \text{on } \Gamma_H. \end{cases}$$

---

## 4. Conclusion and perspectives

In order to model cellular dynamics, a simple model of Fisher-KPP type, considering only the biological effect, was considered in the first step. The comparison of numerical results obtained, in the case where the proliferation and diffusion parameters are constant, with experimental results shows the insufficiency of Fisher-KPP model to accurately represent the activated and inhibited dynamics. Nevertheless, the activation and inhibition operations ( $D$  and  $r$  time-dependent) provide more effective results, which is coherent with the two estimations (3.1) and (3.2).

In order to better model the cellular dynamics, a coupled model is suggested. It consists at the Fisher-KPP equation coupled with the mechanics equation ; the behavior being purely elastic. Moreover, the numerical implementation of such coupled model is in progress.

---

## 5. Bibliographie

- [1] MALANDAIN G., « <https://interstices.info/jcms/i53813/les-mathematiques-cachees-de-la-medecine>. 21/05/2010. »
- [2] PAGE KAREN M., MAINI PHILIP K., A.M. MONK. NICHOLAS, « Complex pattern formation in reaction-diffusion systems with spatially varying parameters », *Physica*, vol. 202, n° , 2005.
- [3] OLSEN L., MAINI P.K., SHERRATT J.A., « Spatially Varying Equilibria of Mechanical Models : Application to Dermal Wound Contraction », *Mathematical Biosciences*, vol. 147, n° 113, 1998.
- [4] FENTEANY G., JANMEY P. A., STOSSEL T. P., « Signaling pathways and cell mechanics involved in wound closure by epithelia cell sheets », *Current Biology*, vol. 10, n° 831, 2000.
- [5] BAO QI., HUGHES R.C., « Galectin-3 and polarized growth within collagen gels of wild-type and ricin-resistant mdck renal epithelial cells », *Glycobiology*, vol. 9, n° 5, 1999.
- [6] QINGHUI MENG, JAMES M. MASON, DEBRA PORTI, ITZHAK D. GOLDBERG, ELIOT M. ROSEN, SAIJUN FAN, « Hepatocyte growth factor decreases sensitivity to chemotherapeutic agents and stimulates cell adhesion, invasion, and migration », *Biochem. Biophys. Res. Commun.*, vol. 274, n° 772, 2000.
- [7] MURRAY J.D., « Mathematical Biology : I. An Introduction, Third Edition », *Springer, Interdisciplinary Applied Mathematics*, vol. 17, 2001.
- [8] MURRAY J.D. , « Mathematical Biology : II. Spatial Models and Biomedical Applications », *Springer, Interdisciplinary Applied Mathematics*, vol. 18, 2011.
- [9] GAFFNEY EAMONN A., MAINI PHILIP K., SHERRATT JONATHAN A., DALE PAUL D., « Wound healing in the corneal epithelium : Biological mechanisms and mathematical models », *J. Theor. Med.*, vol. 1, n° 13, 1997.
- [10] MAINI P.K., OLSEN L., SHERRATT J.A., « Mathematical models for cell-matrix interactions during dermal wound healing », *Int. J. Bifurcation Chaos Appl. Sci. Eng.*, vol. 12, n° 9, 2002.
- [11] PAGE KAREN M., MAINI PHILIP K., MONK NICHOLAS A.M., « Complex pattern formation in reaction-diffusion systems with spatially varying parameters », *Physica D*, vol. 202, n° 95, 2005.
- [12] VEDULA S. R. K., LEONG M. C., LAI T. L. , HERSEN P., KABLA A. J., LIM C.T., LADOUX B., « Emerging modes of collective cell migration induced by geometrical constraints », *PNAS*, vol. 109, 2012.
- [13] LEE P., WOLGEMUTH C. W., « Crawling Cells Can Close Wounds without Purse Strings or Signaling », *PLoS Computational Biology*, vol. 7, 2011.
- [14] SAEZ A., ANON E., GHIBAUDO M., O DU ROURE, MEGLIO J-M DI., HERSEN P., SILBERZAN P., BUGUIN A., LADOUX B., « Traction forces exerted by epithelial cell sheets », *J. Phys. : Condens. Matter*, vol. 22, n° 9, 2010.
- [15] KABLA A. J., « Collective cell migration : leadership, invasion and segregation », *J. R. Soc. Interface*, vol. 9, 2012.
- [16] OLSEN L., MAINI P.K., SHERRATT J.A., « A mechanochemical model for normal and abnormal dermal wound repair », *Nonlinear Analysis, Theory, Methods & Applications*, vol. 30, n° 6, 1997.
- [17] OLSEN L., MAINI P.K., SHERRATT J.A., « A Mechanochemical Model for Adult Dermal Wound Contraction and the Permanence of the Contracted Tissue Displacement Profile », *J. theor. Biol.*, vol. 177, 1995.
- [18] PERELSON A. S., MAINI P. K., MURRAY J. D., HYMAN J. M., OSTER G. F.G. F., « Non-linear pattern selection in a mechanical model for morphogenesis », *Journal of Mathematical*

- biology. Springer Veriag*, vol. 24, n° 525, 1986.
- [19] SHERRATT J. A., « Actin aggregation and embryonic epidermal wound healing », *Journal of Mathematical biology. Springer Veriag*, vol. 31, n° 703, 1993.
  - [20] GOTO Y., « A 2-dimensional mechanical model of the formation of a somite », *International journal of numerical analysis and modeling*, vol. 10, n° 1, 2013.
  - [21] HABBAL A., BARELLI H., MALANDAIN G., « Assessing the ability of the 2D Fisher-KPP equation to model cell-sheet wound closure », *Mathematical Biosciences*, vol. 252, n° 45, 2014.
  - [22] HANSEN C. M. , « Polymer science applied to biological problems : prediction to cytotoxic drug interactions with DNA », *European Polymer Journal*, vol. 44, 2008.
  - [23] HAMEL É. , « Modélisation mathématique de la dépression synaptique et des périodes réfractaires pour le quanton », 2013.
  - [24] YEGANEFAR N., « Définitions et analyse de stabilité pour les systèmes à retard non linéaires », Novembre 2006.
  - [25] BREZIS H., « Analyse fonctionnelle : Théorie et applications », *Dunod*, 1999.
  - [26] RAVIART P.A., THOMAS J.M., « Introduction à l'analyse numérique des équations aux dérivées partielles », *Masson*, 1983.